

Unoccupied bulk, surface, and image states on Ni(001), Ni(111), and Ni(110)

R. F. Garrett*

Department of Materials Science and Engineering, State University of New York, Stony Brook, New York 11794

N. V. Smith

AT&T Bell Laboratories, Murray Hill, New Jersey 07974

(Received 20 September 1985)

A reanalysis of recent inverse-photoemission data on Ni using an empirical band structure shows that the bulk band structure seen in inverse photoemission does not differ significantly from that seen in photoemission. The systematics of surface-state occurrence are in agreement with a recent phase-analysis model. The occurrence of a zone-boundary image state near \bar{Y} for Ni(110) is discussed. Its relatively flat dispersion curve is predicted by the phase model and is dominated by perpendicular effects rather than surface corrugation.

I. INTRODUCTION AND CONCLUSIONS

The photoemission properties of metallic Ni are especially interesting since they display significant departures from the expectations of first-principles one-electron band theory. The d band has a narrower width than predicted, and it sits higher in energy with respect to the s - p manifold; also the exchange splitting is smaller than predicted.¹ Photoemission work has recently been supplemented by extensive inverse photoemission measurements² of the unoccupied states. Reference 2 reports a comparison between the experimental results and the predictions of a first-principles band calculation, and "good agreement is found for the energies of bulk interband transitions." If experimentally significant, this conclusion would be of considerable theoretical importance since it would imply that inverse photoemission from Ni is well described by first-principles band theory, whereas ordinary photoemission is not.

In this paper we describe a separate analysis of the inverse photoemission data of Ref. 2 using an empirical band structure which has been adjusted to achieve agreement with ordinary photoemission data.³ We find that only a few of the observed spectral features can be identified exclusively as bulk derived, and that within the current limitations of experimental resolution the band structure seen in inverse photoemission does not differ from that seen in photoemission.

The Ni spectra of Ref. 2 display an abundance of peaks which are surface derived or which are composites of surface-derived and bulk-derived features. These features and their energy locations are reasonably well reproduced by a simple multiple-reflection (or phase-analysis) model which has been found previously to work very well in the description of surface-state occurrence on the low index faces of Cu.^{4,5}

A feature found on Ni which is not found in Cu is an image state at the zone boundary point \bar{Y} on the (110) face. We show that this state and its energy dispersion are also well described by the phase-analysis model. The band gap between image states at the zone boundary is due pri-

marily to effects associated with the perpendicular registry of the image-state wave function with respect to the atomic layers, and only slightly to surface corrugation.

II. BULK-BAND-STRUCTURE DISCUSSION

A. Empirical bands

The band structure used here is a combined interpolation scheme⁶ whose parameters have been adjusted to bring about agreement with angle-resolved photoemission data.⁷ The details of the adjustments are to be found in Ref. 3. The adjustment of most relevance here is a *downward* shift of the s - p bands relative to the d band and Fermi level E_F .

Assuming bulk direct transitions, we calculate the final-state isochromat dispersion curves⁸ $E_f(k_{||})$ for transitions satisfying the direct transition condition

$$E_i(\mathbf{k}) - E_f(\mathbf{k}) - \hbar\omega = 0. \quad (1)$$

We consider transitions from initial band $i=7,8,9$ into final-state band $f=6$ in the energy range up to 7 eV above E_F . Because of the empirical adjustments mentioned above, and because we shall not be primarily concerned with the d band, values of E_i and E_f will generally be lower than those obtained from a first-principles band calculation. Calculations will be shown only for the minority-spin band structure. $E_f(k_{||})$ isochromats for the majority spins lie, in some places, lower than for the minority spins (by $\lesssim 60$ meV) due to differential s - d hybridization.⁹

B. Comparison with experiment

A grand summary of the data of Goldmann *et al.*² is compared with our various theoretical predictions in Fig. 1. Solid circles represent those experimental peaks which are unambiguously bulk derived. Solid and dashed curves are the $E_f(k_{||})$ isochromats for the kinematically allowed transitions. Solid curves indicate large coupling probability (large c_i in the terminology of Ref. 8) for the incoming

electron. On all faces a peak is seen at about 0.3 eV above E_F , which is identified with transitions into the unoccupied minority-spin d band (no calculation shown). This is well understood and will not be considered further here.

On Ni(001), the peak designated B_2 is in good overall agreement with a close-lying theoretical isochromat curve. The agreement represents an improvement over that reported in Ref. 2, and indicates that photoemission and inverse photoemission detect the same effective band structure. However, it has to be recognized that on Ni(001), just as on Cu(001),⁴ there is the strong probability of a

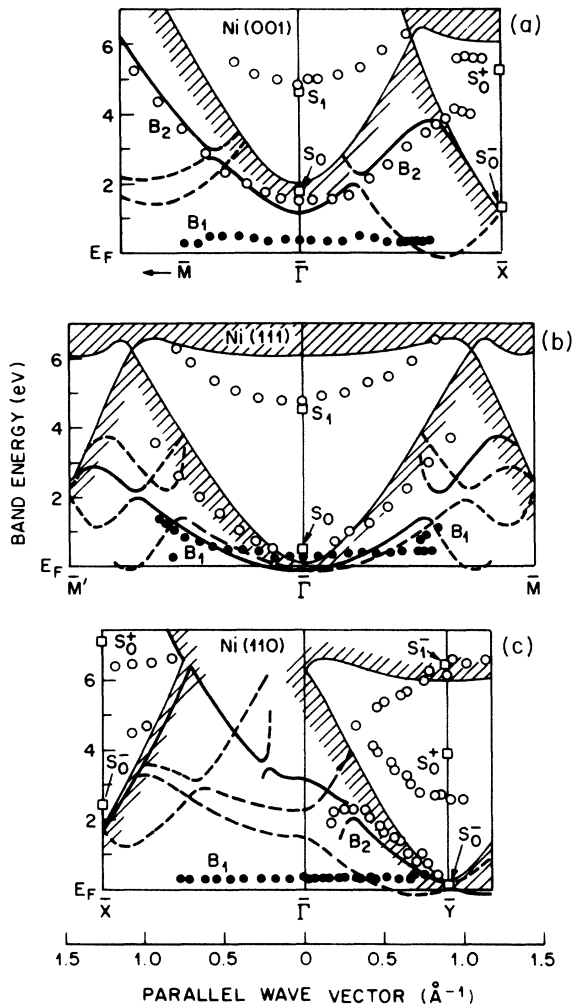


FIG. 1. Comparison between theory and experiment for the energies and k_{\parallel} dispersions of bulk and surface states on low index Ni faces. Hatching indicates the projection of the bulk band structure. Experimental data is from Goldmann *et al.* (Ref. 2): solid circles denote peaks which are unambiguously bulk derived; open circles denote surface-derived or composite bulk and/or surface features. Solid and dashed curves are the theoretical $E_F(k_{\parallel})$ isochromats due to direct transitions; solid curves distinguish the isochromats associated with good coupling to incoming electrons. Data points and curves apply to photon energies 9.7, 9.7, and 9.5 eV for Ni(001), Ni(111), and Ni(110), respectively. Open squares indicate the energies of the surface states and resonances S_n^{\pm} generated by the heuristic phase model.

surface resonance having approximately the same energy and same energy dispersion.

On Ni(111), the comparison with theory for peak B_1 is satisfactory along the $\bar{\Gamma}\bar{M}'$ azimuth but unsatisfactory along $\bar{\Gamma}\bar{M}$. The difficulties here appear to be associated more with resolving the s - p feature from the d feature rather than with any fundamental problem with the band structure.

On Ni(110), feature B_2 can be identified with a theoretical curve, but the agreement is less perfect than that reported in Ref. 2. Once again, however, there is the strong likelihood that this is a composite structure incorporating a surface resonance expected near \bar{Y} .

To summarize this bulk-band-structure discussion, we find no compelling evidence that the band structure seen in inverse photoemission differs from that seen in photoemission. This remains, however, an interesting theoretical point worthy of further investigation. It would be desirable to perform experiments at higher resolution and at higher photon energies in order to remove the near degeneracies between bulk-derived and surface-derived features.

III. SURFACE-STATE DISCUSSION

A. Phase model

The systematics of surface-state occurrence in nearly-free-electron (NFE) band gaps can be described by a heuristic phase analysis^{4,5} based on multiple reflection theory.¹⁰ If $r_C e^{i\phi_C}$ and $r_B e^{i\phi_B}$ represent the reflectance of the electron wave at the crystal and surface barriers, respectively, bound states occur when the condition

$$\phi_B + \phi_C = 2\pi n, \quad n=0,1,2,\dots \quad (2)$$

is satisfied. We have applied this phase model to five gaps distributed over the three low index faces of Ni. For ϕ_B we have used the empirical form proposed for Cu in Ref. 5 scaled to the slightly different inner potential for Ni. For ϕ_C we have used NFE expressions based on the in-layer termination of Ref. 5. The NFE band gap parameter $2V_g$ of the model was fitted to the experimental $L_3 \rightarrow L_1$ gap for the Ni(111) $\bar{\Gamma}$, Ni(110) \bar{Y} , and Ni(001) \bar{X} cases,¹¹ and to the $X'_4 \rightarrow X_1$ gap for the Ni(001) $\bar{\Gamma}$ and Ni(110) \bar{X} cases. In the zone-boundary cases, there are two branches ϕ_C^+ and ϕ_C^- depending on whether the wave function in the crystal is of even or odd symmetry with respect to surface atoms:

$$\psi^+ = e^{qz} \cos(k_{\parallel} r_{\parallel}) \cos(pz + \delta) \quad (s_{\parallel}\text{-like}), \quad (3)$$

$$\psi^- = e^{qz} \sin(k_{\parallel} r_{\parallel}) \sin(pz + \delta) \quad (p_{\parallel}\text{-like}). \quad (4)$$

As discussed in Ref. 5, these states will differ in energy because of the surface corrugation potential.

B. Comparison with experiment

Energies predicted by the phase model are compared with experiment in Fig. 1. The surface states or resonances are designated S_n^{\pm} , where the superscript (where appropriate) denotes wave-function parity, and the sub-

script can be either $n=0$ for crystal-induced states of the Shockley type or $n=1$ for the first member of the Rydberg series of image states.

At $\bar{\Gamma}$ on Ni(001) and Ni(111), S_1 image states are predicted with binding energies relative to the vacuum level of 0.6 and 0.8 eV. The experimental values² are 0.4 ± 0.2 and 0.6 ± 0.2 eV.

The S_0 resonance at Ni(001) $\bar{\Gamma}$ is presumably buried under the bulk-derived B_2 peak. A similar situation prevails at Cu(001) $\bar{\Gamma}$, although the S_0 resonance has recently been separated.¹² The S_0 state at Ni(111) $\bar{\Gamma}$ correlates well with a set of experimental points in Fig. 1 which are well separated from any bulk direct transition. As indicated by Goldmann *et al.*,² this peak (S_1 in their terminology) is unambiguously a surface-derived feature. Its analog at Cu(111) $\bar{\Gamma}$ (Refs. 4 and 13) and Ag(111) $\bar{\Gamma}$ (Ref. 14) is well established, and it may have been observed also at Pd(111) $\bar{\Gamma}$.¹⁵ A one-step treatment of the S_0 state at Ni(111) $\bar{\Gamma}$ has been reported by Borstel *et al.*¹⁶

The $p_{||}$ -like S_0^- zone-boundary state has not yet been seen at Ni(001) \bar{X} or Ni(110) \bar{X} although these states are seen in Cu.^{17,18} The S_0^- resonance at Ni(110) \bar{Y} correlates well with the nearby B_2 experimental peak, leading us to propose that that peak is a composite bulk-surface feature. Its analog is well established at Cu(110) \bar{Y} (Ref. 19) and at Ag(110) \bar{Y} (Ref. 20). The $s_{||}$ -like S_0^+ states are seen in all the zone-boundary gaps considered here.

IV. ZONE-BOUNDARY IMAGE STATES

A. Phase analysis

The only empty surface feature seen so far on Ni which is not seen on Cu is the S_1^- image state at Ni(110) \bar{Y} . It is

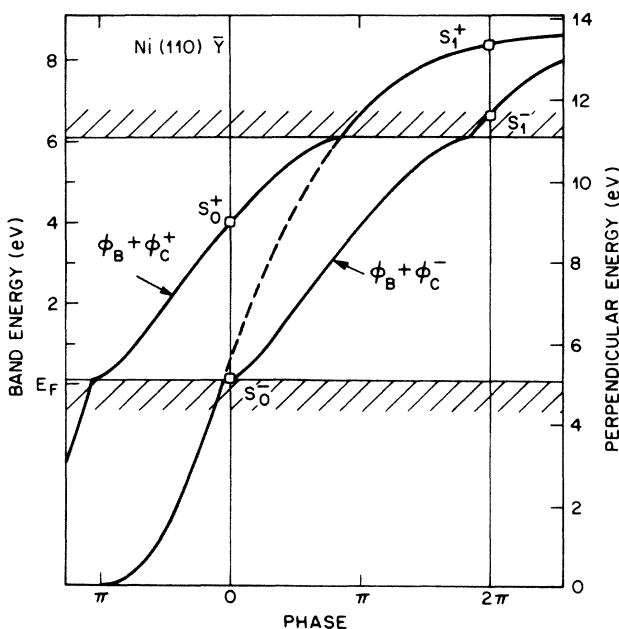


FIG. 2. Energy variation of the round-trip reflection phase accumulation $\phi_B + \phi_C^\pm$ appropriate to the \bar{Y} point on Ni(110). Open squares indicate the solutions for bound surface states or resonances.

therefore worthy of extended discussion. The way in which two surface states can arise at the zone boundary in the case of a step barrier has been discussed by Bartynski *et al.*²¹ These states correspond to the $n=0$ states, S_0^- and S_0^+ in the present terminology. The way in which the phase model generates image states is illustrated in Fig. 2. The gap at Ni(110) \bar{Y} is sufficiently wide and sufficiently high in energy that an additional state (actually a resonance just outside the gap) is generated due to the rapid variation of ϕ_B for an image barrier. This zone boundary S_1^- state is particularly interesting. It is an image state having its main wave-function amplitude well outside the crystal. Its registry with respect to the surface is $p_{||}$ -like, in the sense that the nodes in the lateral dependence of its wave function occur directly above rows of surface atoms. The phase model predicts the existence of a similar S_1^- image state at Ni(110) \bar{X} at about 10.2 eV above E_F . It would be worth searching for experimentally.

B. Energy dispersion

The experimental dispersion of the S_1^- image state has been fitted with a relatively large effective mass $m^*/m = 1.7 \pm 0.3$, which has been attributed to the effects of surface corrugation.^{2,22} We show that this flat dispersion is well accounted for by the phase model. Surface corrugation is involved to a small extent, but this arises naturally out of the phase model and does not have to be invoked as a separate mechanism.

For reasons of convenience and simplicity, we use here the WKB image form for ϕ_B rather than the empirical form used above. The WKB image form for ϕ_B is written²³

$$\phi_B/\pi = [(3.4 \text{ eV})/(E_V - \epsilon)]^{1/2} - 1, \quad (5)$$

where E_V is the vacuum energy and ϵ is the perpendicular kinetic energy. The energies of the image states now take the following convenient forms:

$$E = E_V - e_n + \hbar^2 k^2 / 2m, \quad (6)$$

$$e_n = (0.85 \text{ eV}) / (n+a)^2, \quad n = 1, 2, \dots \quad (7)$$

$$a = \frac{1}{2}(1 - \phi_C^\pm/\pi). \quad (8)$$

In going from the bottom to the top of the Shockley-inverted gap at \bar{Y} on Ni(110), ϕ_C^- increases from a value near $\pi/2$ to a value near $3\pi/2$, and thus the binding energy e_1 increases from 0.5 to 1.5 eV. The associated increase of 1.0 eV in the value of e_1 serves to flatten the free-electron dispersion relation of Eq. (6). We have not attempted a detailed calculation here, but have merely sketched in the outlines of such a calculation in Fig. 3 using Eqs. (5)–(8) and noting that $\phi_C^\pm \simeq \pi/2$ above the top of the gap. The comparison between the elementary phase analysis and the experimental data of Ref. 2 is also shown in Fig. 3. Agreement is better than expected given the extreme simplicity of the theoretical model.

Note that the dispersion relation is not parabolic so that it is not meaningful to fit the data with an effective mass. The flattening of the dispersion relation is due to the $k_{||}$ dependence of e_1 , and this is a “crystal-induced” effect since it derives from the reflection properties of the bulk band gap. A related effect, noted in Ref. 5, is the tenden-

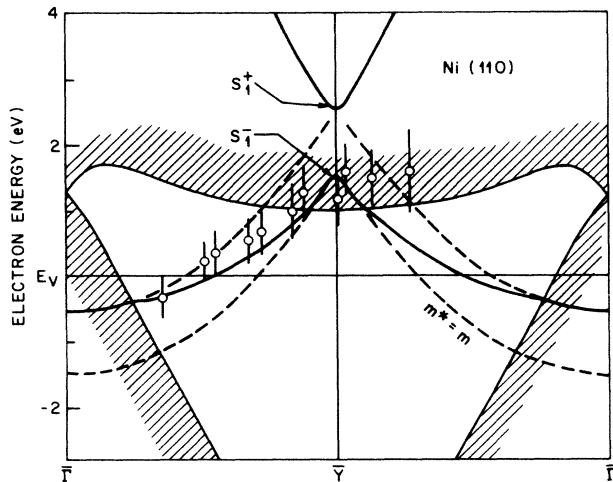


FIG. 3. $E(k_{\parallel})$ dispersion relations for the $n=1$ image state near Ni(110) \bar{Y} . Bold curves represent the prediction of the most elementary phase model. The dashed curves are free-electron parabolas originating from binding energies $e_1=0.54$ and 1.51 eV. Energies are expressed relative to the vacuum level E_V .

cy of a surface state or image state falling close to a projected band edge to track that band edge. If the band edge is flat, the apparent effective mass will be large. The S_1 image state on Ni(111) ($m^*/m = 1.6 \pm 0.2$, Ref. 2) is a candidate for this effect.

C. Nature of the gap

The nature of the $S_1^- \rightarrow S_1^+$ band gap at \bar{Y} is interesting in that it has both parallel and perpendicular aspects. S_1^- is p_{\parallel} -like and S_1^+ is s_{\parallel} -like. Since the pseudopotential for a Shockley-inverted gap is repulsive ($V_g > 0$), S_1^- will lie lower in energy than S_1^+ . This purely lateral effect can be

termed the "surface corrugation" effect. In addition, however, there is a perpendicular effect. In Eqs. (3) and (4) we have $\delta=0$ above the top of the gap. Thus ψ^- is p_{\perp} -like in the sense that it places its nodes on successive atomic layers. ψ^+ is s_{\perp} -like. This will also have the effect of placing S_1^- lower in energy than S_1^+ . We have not isolated these separate contributions to the band gap, but it is reasonable to suppose that they are roughly equal and small.²⁴ These two contributions to the $S_1^- \rightarrow S_1^+$ gap relate only to the low-amplitude part of the wave function residing within the crystal.

The dominant contribution to the $S_1^- \rightarrow S_1^+$ gap relates to the large part of the $n=1$ wave-function amplitude which resides outside the image plane. Since $\phi_C^- - \phi_C^+ = \pi$, the effect is to push the main wave-function amplitude of the S_1^+ state further away from the crystal, where it experiences a weaker image potential than the S_1^- state. Thus S_1^+ lies higher in energy than S_1^- , and this is the principal contribution to the gap. This is a "perpendicular effect" since it relates to the distance of the main wave-function amplitude from the crystal surface. Note that the detailed properties of the crystal are largely irrelevant. The only role of the crystal is to provide a band gap and values of ϕ_C^- and ϕ_C^+ differing by π , a function of symmetry rather than specific properties of the crystal. The magnitude of the gap is therefore determined primarily by the energy dependence of ϕ_B . It would be interesting, using inverse photoemission spectroscopy, to try to measure the $S_1^- \rightarrow S_1^+$ gap. This would provide valuable information on the image barrier potential, but rather little information on the substrate.

ACKNOWLEDGMENTS

One of us (R.F.G.) is supported by the U.S. Department of Energy under Contract No. DE-AC02-80ER10750.

*Present address: National Synchrotron Light Source, Brookhaven National Laboratory, Upton, NY 11973.

¹For an historical summary and discussion, see N. V. Smith, R. Lässer, and S. Chiang, Phys. Rev. B 25, 793 (1982), and references therein.

²A. Goldmann, M. Donath, W. Altmann, and V. Dose, Phys. Rev. B 32, 837 (1985).

³N. V. Smith, R. Lässer, and S. Chiang, Phys. Rev. B 25, 793 (1982).

⁴S. L. Hulbert, P. D. Johnson, N. G. Stoffel, W. A. Royer, and N. V. Smith, Phys. Rev. B 31, 6815 (1985).

⁵N. V. Smith, Phys. Rev. B 32, 3549 (1985).

⁶N. V. Smith, Phys. Rev. B 19, 5019 (1979).

⁷F. J. Himpsel, J. A. Knapp, and D. E. Eastman, Phys. Rev. B 19, 2919 (1979); W. Eberhardt and E. W. Plummer, *ibid.* 21, 3245 (1980).

⁸D. P. Woodruff, N. V. Smith, P. D. Johnson, and W. A. Royer, Phys. Rev. B 26, 2943 (1982).

⁹A. Seiler, C. Feigerle, R. Celotta, D. T. Pierce, and N. V. Smith (unpublished).

¹⁰P. M. Echenique and J. B. Pendry, J. Phys. C 11, 2065 (1978);

E. G. McRae, Surf. Sci. 25, 491 (1971).

¹¹The bottom of the L gap at Ni(111) $\bar{\Gamma}$ is therefore d -like rather than p -like. The phase ϕ_C , however, must still increase by π on traversing such a gap. Also, at Ni(001) \bar{X} , the bottom of the projected band gap does not correspond to the L_2 point, but to the "A" point as discussed for the case of Cu(001) \bar{X} by S. D. Kevan, N. G. Stoffel, and N. V. Smith, Phys. Rev. B 31, 3348 (1985).

¹²D. P. Woodruff, S. L. Hulbert, P. D. Johnson, and N. V. Smith, Phys. Rev. B 31, 4046 (1985).

¹³P. O. Gartland and B. J. Slagsvold, Phys. Rev. B 12, 4047 (1975).

¹⁴H. F. Roloff and H. Neddermeyer, Solid State Commun. 21, 561 (1977).

¹⁵D. A. Wesner, P. D. Johnson, and N. V. Smith, Phys. Rev. B 30, 503 (1984).

¹⁶G. Borstel, G. Thörner, M. Donath, V. Dose, and A. Goldmann, Solid State Commun. 55, 469 (1985).

¹⁷S. D. Kevan, Phys. Rev. B 28, 2268 (1983).

¹⁸R. A. Bartynski and T. Gustafsson (unpublished).

¹⁹S. D. Kevan, Phys. Rev. B 28, 4822 (1983); D. G. Dempsey

- and L. Kleinman, *ibid.* **16**, 5356 (1977).
- ²⁰K. M. Ho, B. N. Harmon, and S. H. Liu, *Phys. Rev. Lett.* **44**, 1531 (1980); for a discussion of unoccupied surface states on Ag(110), see B. Reihl, R. R. Schittler, and H. Neff, *Phys. Rev. Lett.* **52**, 1826 (1984).
- ²¹R. A. Bartynski, T. Gustafsson, and P. Soven, *Phys. Rev. B* **31**, 4745 (1985).
- ²²N. Garcia, B. Reihl, K. H. Frank, and A. R. Williams, *Phys. Rev. Lett.* **54**, 591 (1985).
- ²³E. G. McRae, *Rev. Mod. Phys.* **51**, 541 (1979); E. G. McRae and M. L. Kane, *Surf. Sci.* **108**, 435 (1981).
- ²⁴The inherent smallness of the effect of surface corrugation on the effective mass is discussed by S. L. Hulbert, P. D. Johnson, M. Weinert, and R. F. Garrett, *Phys. Rev. B* **33**, 760 (1986); J. B. Pendry, C. G. Larsson, and P. M. Echenique, *Surf. Sci.* (to be published); see also, W. L. Clinton, M. A. Esrick, and W. S. Sacks, *Phys. Rev. B* **31**, 7540 (1985).